Supporting Information

Three-Dimensional Plasmonic Nanocluster-Driven Light-Matter Interaction for Photoluminescence Enhancement and Picomolar-Level Biosensing

Won-Geun Kim[1,2,†], Jong-Min Lee[1,3,†], Younghwan Yang[2,†], Hongyoon Kim[2], Vasanthan Devaraj[1], Minjun Kim[4], Hyuk Jeong[1], Eun-Jung Choi[1], Jihyuk Yang[5], Yudong Jang[6], Trevon Badloe[2], Donghan Lee[4], Junsuk Rho[2,7,8,], Ji Tae Kim[5,*] and Jin-Woo Oh[1,9,*]*

[1]BIT Fusion Technology Center, Pusan National University, Busan 46241, Republic of Korea

[2]Department of Mechanical Engineering, Pohang University of Science and Technology (POSTECH), Pohang 37673, Republic of Korea

[3]Center of Nano Convergence Technology and School of Nanoconvergence Technology, Hallym University, Chuncheon 24252, Republic of Korea

[4]Department of Physics, Chungnam National University, Daejeon 34134, Republic of Korea

[5]Department of Mechanical Engineering, The University of Hong Kong, Pokfulam Road, Hong Kong, China

[6]Institute of Quantum Systems (IQS), Chungnam National University, Daejeon 34134, Republic of Korea

[7]Department of Chemical Engineering, Pohang University of Science and Technology (POSTECH), Pohang 37673, Republic of Korea

[8]POSCO-POSTECH-RIST Convergence Research Center for Flat Optics and Metaphotonics, Pohang 37673, Republic of Korea.

[9]Department of Nanoenergy Engineering, Pusan National University, Busan 46241, Republic of Korea

[†]*These authors contributed equally to this work.*

**Corresponding author E-mail:* ojw@pusan.ac.kr *(J.-W. Oh),* jtkim@hku.hk *(J. T. Kim),* jsrho@postech.ac.kr *(J. Rho)*

Supplementary Discussion 1. Effective medium theory.

To estimate the complex refractive indices of inks, we use two types of effective medium theory, the Bruggeman-mixing formula (Details in Results and discussion) and the Parallel effective medium approximation ($\tilde{n}_{Par}$) which is given as follows:[1]

$$\tilde{n}_{Par} = f_{\mathrm{PVP}}\sqrt{\varepsilon_{\mathrm{PVP}}} + f_{\mathrm{PVP}}\sqrt{\varepsilon_{\mathrm{Au}}} \quad \text{(S.1)}$$

Since there are no explicit criteria as for which approximation is valid[2], we also display the calculated effective refractive index spectra using Parallel effective medium approximation. Although the calculated refractive indices with the two models show a minor discrepancy at f_{Au} = 0.55 due to the inherent limitation of current effective medium theories[3], the similar trends confirm the reliability of the estimated complex refractive index.

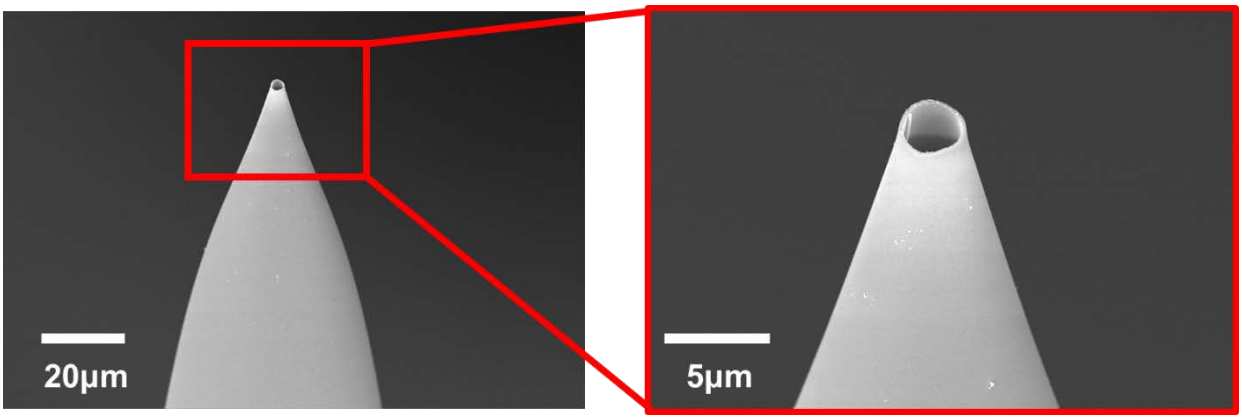

Figure S1. SEM images of a micropipette used for the self-assembly of 3D plasmonic structures.

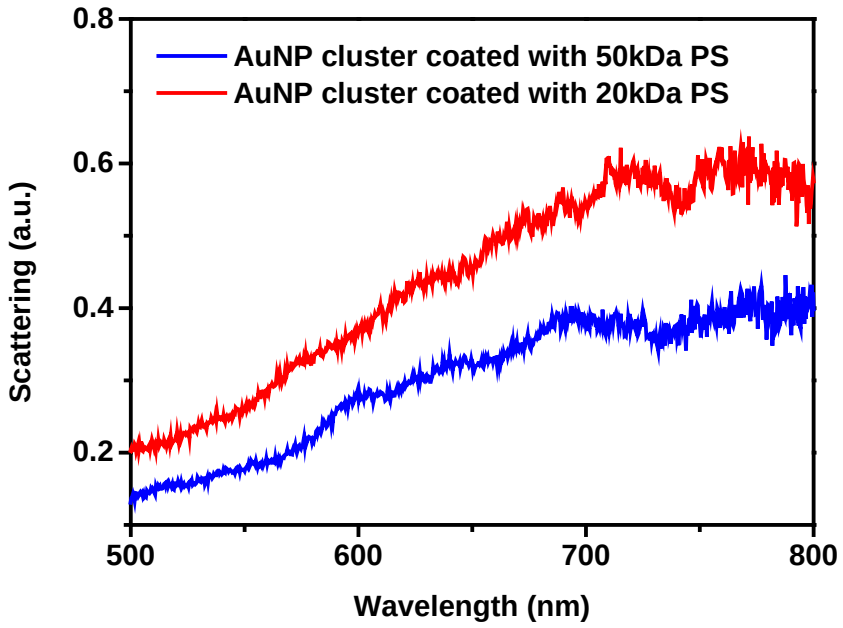

Figure S2. Scattering spectra of 3D plasmonic structures consisting of 100 nm AuNPs coated with polystyrene (PS).

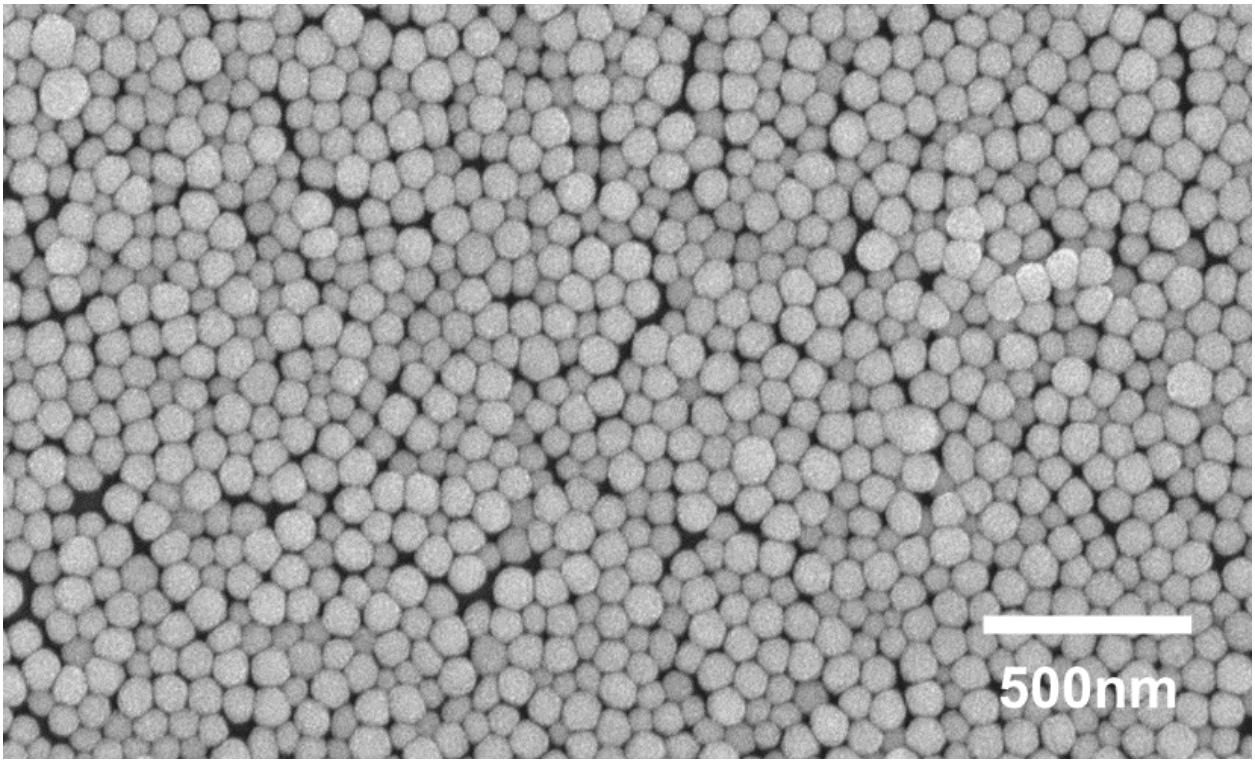

Figure S3. Deposited single layer of AuNPs on a glass substrate.

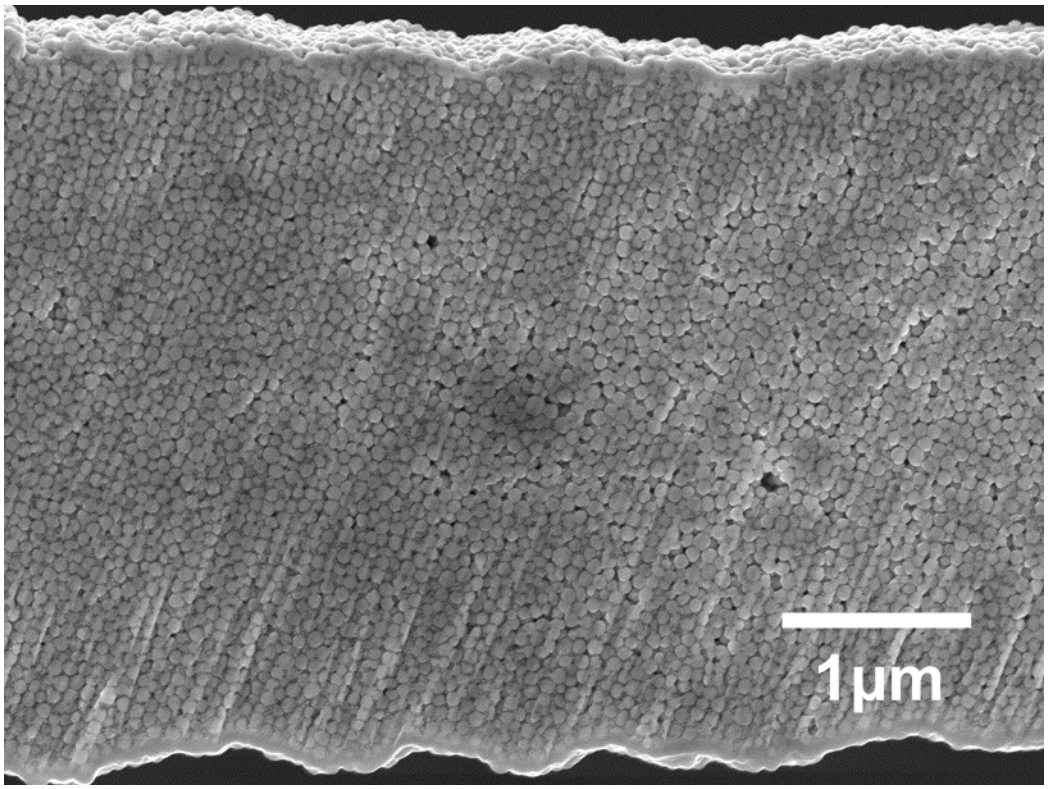

Figure S4. SEM image of a cross section of a 3D plasmonic micropillars.

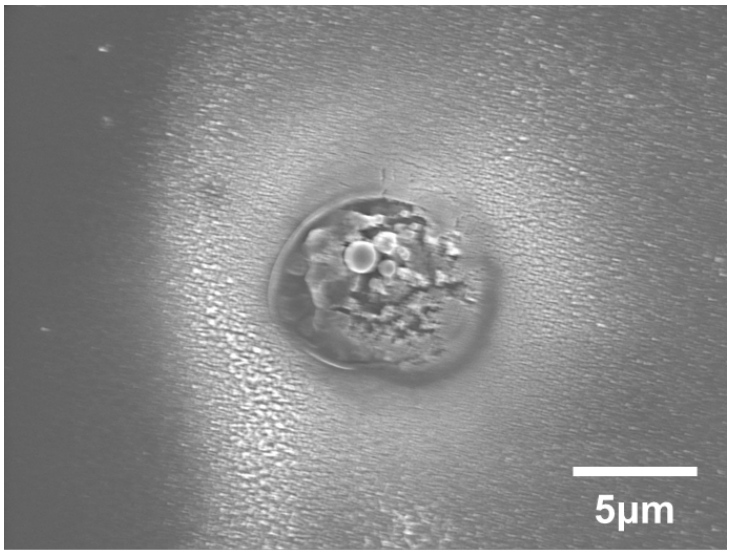

Figure S5. SEM image of a collapsed QD-embedded heterogeneous 3D plasmonic structures.

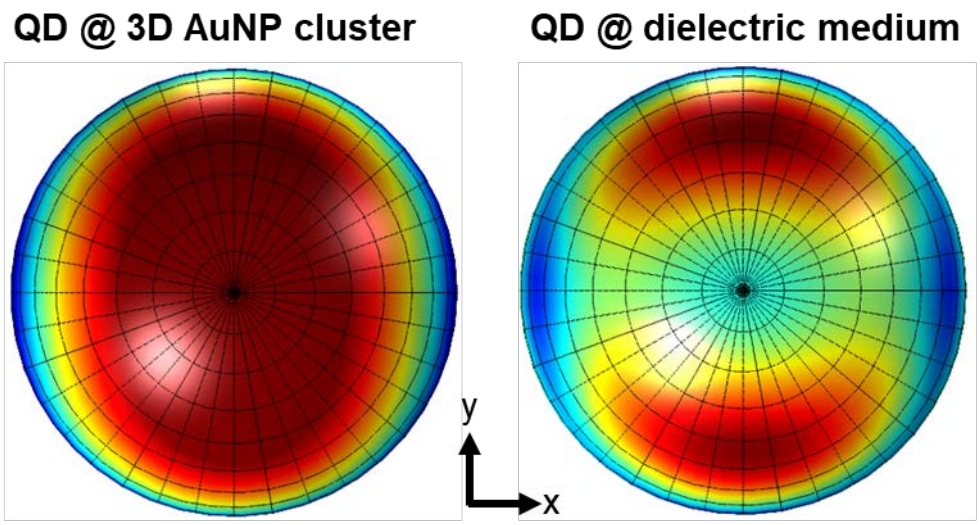

Figure S6. Simulation results of the far-field characteristics of QD-embedded 3D AuNP cluster and dielectric medium.

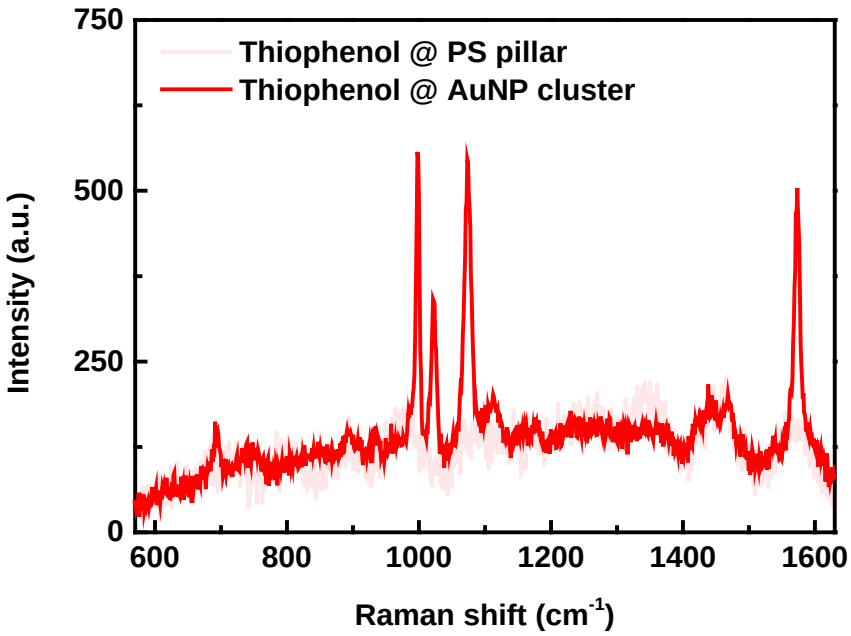

Figure S7. SERS spectra of thiophenol embedded in AuNP cluster and PS pillars.

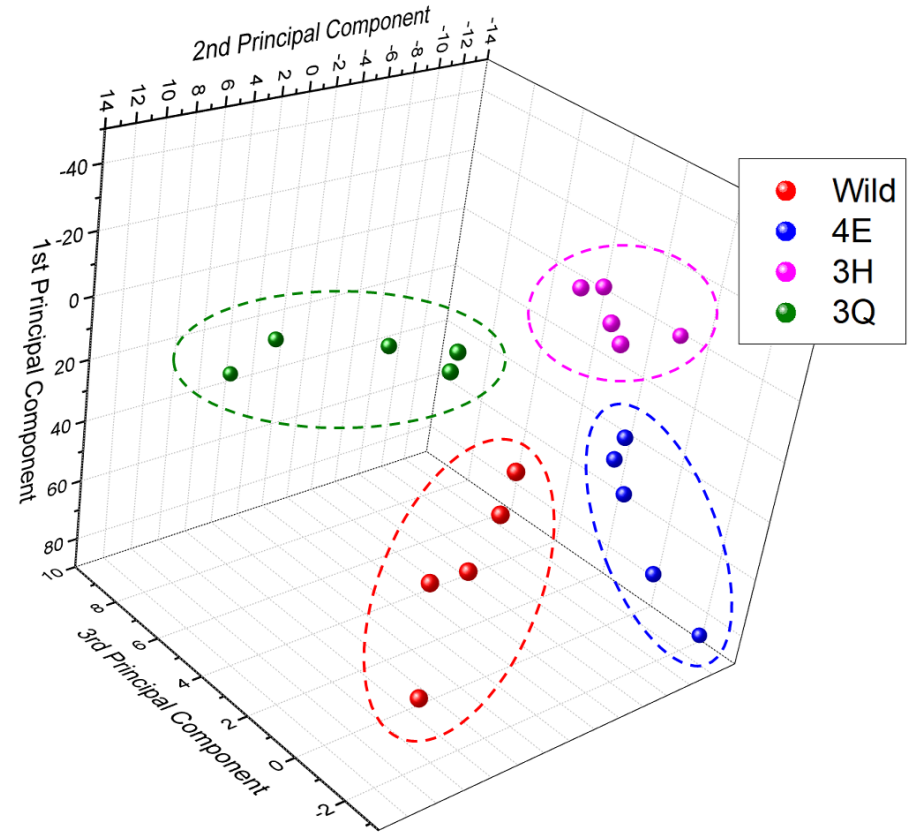

Figure S8. Principal component analysis (PCA) performed on Raman spectra of various mutant M13 bacteriophage. From the PCA, we can discriminate information about the relative importance of the variance values. The largest variance corresponds to the 1st principal component, the second largest one corresponds to the 2nd principal component and the third largest one corresponds to the 3rd principal component. The value of variation in the PCA indicates the contributions of each discriminant factor to the total variance of the coordinates. We categorized the points for each of the virus types,es, including wild, 4E , 3H and 3Q. Through such categorization, we can confirm the discrimination capability and high reproducibility of the characteristic SERS signal on the embedded virus.

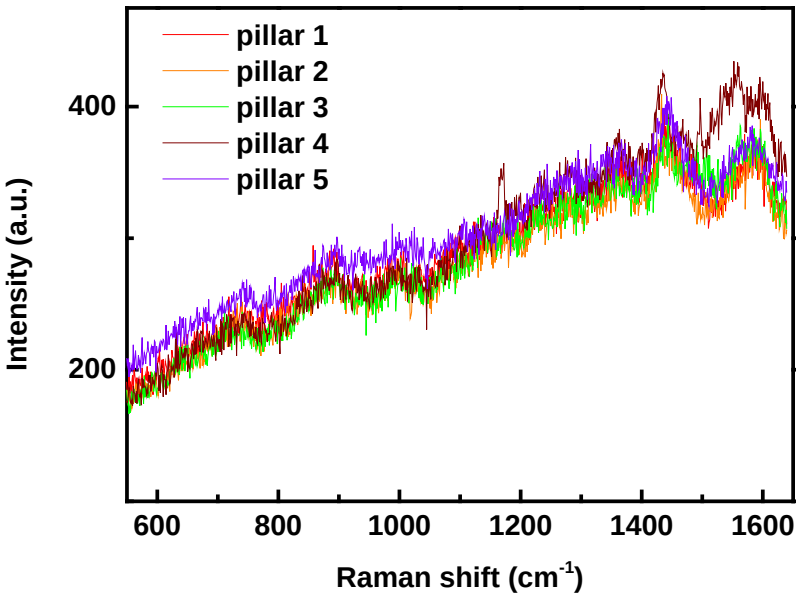

Figure S9. Raman spectra of WT phages embedded in five individual 3D plasmonic pillars.

Supplementary References

(1) Taylor, D. J.; Fleig, P. F.; Hietala, S. L. Technique for characterization of thin film. *Thin Solid Films* **1998**, *332*, 257-261.

(2) Braun, M. M.; Pilon, L. Effective Optical Properties of Non-absorbing Nanoporous Thin-Films. *Thin Solid Films* **2006**, *496*, 505-514.

(3) Garahan, A.; Pilon, L.; Yin, J. Effective Optical Properties of Absorbing Nanoporous and Nanocomposite Thin Films. *J. Appl. Phys.* **2007**, *101*, 014320.